

Charge-transfer multiplet analysis of the resonant $2p3p3p$ Auger spectra of CaF_2

F.M.F. de Groot*

Solid State Physics Laboratory, University of Groningen, Nijenborgh 4, 9747 AG Groningen, The Netherlands

R. Ruus

Institute of Physics, Estonian Academy of Sciences, Riia 142, EE2400, Tartu, Estonia

M. Elango†

Department of Atomic Spectroscopy, Lund University, Sölvegatan 14, S-223 62 Lund, Sweden

(Received 19 December 1994)

A theoretical description is given of the $2p3p3p$ ($= L_{2,3}M_{2,3}M_{2,3}$) resonant Auger spectra in CaF_2 . Using a charge-transfer multiplet analysis, it is shown that the $2p3p3p$ Auger spectra excited at the $2p$ x-ray absorption edge show a large variation if one scans through the edge and excites the different symmetry states. A detailed comparison is made with experiment. The origins of the symmetry effects on the resonance are analyzed and the full charge-transfer multiplet theory is approximated using crystal-field and atomic multiplet calculations. The analysis shows that the Auger spectra of CaF_2 are dominated by the resonance channel, with little contribution of the normal Auger channel. The differences with other recently used analysis are discussed.

I. INTRODUCTION

Resonant $2p3p3p$ Auger spectroscopy has been studied experimentally for KF , KCl , CaF_2 , CaCl_2 , and Sc_2O_3 .¹ Scanning through the $2p$ x-ray absorption edge the $2p3p3p$ Auger spectra are detected. CaF_2 , as well as the other compounds mentioned, is an insulator and has a gap of 12 eV in between the filled $F p$ band and the $\text{Ca } 3d$ (and $4sp$) band. The Ca atoms are surrounded by a cube of eight F atoms. The $2p$ x-ray absorption spectrum of CaF_2 has been measured with high-resolution and analyzed successfully using a crystal-field multiplet model.² In the crystal-field multiplet model the initial state is described in the ionic limit as $3d^0$ with $2p^53d^1$ final states. The $2p$ x-ray absorption spectrum of CaF_2 consists of four peaks and small prepeaks and the crystal-field multiplet analysis shows that there are in total seven transitions due to the ($2p3d; 2p3d$) Coulomb and exchange matrix elements in the final state, which causes transitions which are forbidden in a single particle scheme.^{2,3}

In the resonant $2p3p3p$ Auger experiments the excitation energy is varied through the edge and $2p3p3p$ Auger spectra are measured for the different $2p^53d^1$ excitonic states. The interpretation of the equivalent spectra of KCl showed that the $2p3p3p$ Auger peaks reveal states of both constant kinetic energy and constant binding energy (see Fig. 8 in Ref. 1). The constant binding-energy peaks indicate so-called spectator $2p3p3p$ Auger transitions, in which the $3d^1$ electron remains present in the final state.¹ A theoretical analysis of resonant $2p3p3p$ Auger spectroscopy has been recently given by both Kuk *et al.* for KF (Ref. 4) and by Tanaka and Jo for a series of transition metal oxides.⁵ Kuk *et al.* distinguish between normal Auger, spectator Auger, and shake-up Auger. The shake-up Auger is the process in which the spectator $3d$ electron transfers into a $4d$ elec-

tron at the Auger step. Using the ionic approximation, the three processes are normal Auger, $2p^5 \rightarrow 3p^4\varepsilon_p$; spectator Auger, $2p^53d^1 \rightarrow 3p^43d^1\varepsilon_p$; and shake-up Auger, $2p^53d^1 \rightarrow 3p^44d^1\varepsilon_p$. ε_p denotes a free electron of p symmetry. To describe the transitions atomic multiplets are used for the final states. The variations through the x-ray absorption spectrum are explained from a variation in strength of all transitions, which are fitted to experiment.⁴ The approach used by Tanaka and Jo is different. They use only the spectator Auger process and describe the initial state of TiO_2 as a mixture of $3d^0$ and $3d^1\bar{L}$. In the second configuration a hole is created in the oxygen $2p$ band and the electron is added to the $\text{Ti } 3d$ band, which names the model as a “charge-transfer multiplet model”.^{5,6} This costs an energy Δ . By mixing both configurations a ground state with lower energy is formed. A similar approach is then used for the intermediate $2p^53d^1$ states and the final $3p^43d^1$ states. Using this approach they predict a large variation in the $2p3p3p$ Auger spectra of TiO_2 .⁵ The two approaches can be written as normal plus spectator plus shake-up Auger, with an atomic Hamiltonian;⁴ only spectator Auger, with a charge-transfer Hamiltonian.⁵

In the rest of the paper we will analyze these two approaches. In Sec. II we perform charge-transfer multiplet calculations for CaF_2 to explain its resonant $2p3p3p$ Auger spectra. In Sec. III we will analyze the main cause for the observed spectral variations. We discuss the analogy between shake-up processes and the charge-transfer multiplet model and we discuss the Coster-Kronig decay model for ionic insulators such as CaF_2 .

II. CALCULATIONS

The calculations have been performed with a series of programs related to, respectively, atomic multiplet the-

ory, crystal-field multiplet theory, and charge-transfer multiplet theory. The used computer codes are, respectively, the RCG9,⁷ RACAH,⁸ and BANDER (Ref. 9) program in the versions written and/or modified by Thole and co-workers.^{9,10} The Hamiltonian of atomic multiplet theory describes all partly filled bands. For the present problem we have a core state of p symmetry and a valence state of d symmetry. Following the notation of Ref. 6, the Hamiltonian is, in second quantization, written as

$$\begin{aligned} \mathcal{H}_{AM} = & \sum_{(4)} g_{dd} d_1^\dagger d_2^\dagger d_3 d_4 + \zeta_d \sum_{(2)} \mathbf{1} \cdot \mathbf{s} d_1^\dagger d_2 \\ & + \sum_{(4)} g_{pp} p_1^\dagger p_2^\dagger p_3 p_4 + \zeta_p \sum_{(2)} \mathbf{1} \cdot \mathbf{s} p_1^\dagger p_2 \\ & + \sum_{(4)} g_{pd} d_1^\dagger p_2^\dagger p_3 d_4. \end{aligned}$$

The g_{dd} term defines all two-electron integrals, coupling two d electrons. It contains the Coulomb terms F^2 and F^4 . $\sum_{(4)}$ denotes the summation over the four symmetries of the d electrons. ζ_d defines the spin-orbit coupling. The same two terms are repeated for the p state. The last line contains the two-electron integrals coupling the p state with the d state, represented with the Coulomb (F^2) and exchange (G^1, G^3) integrals.

The crystal-field Hamiltonian is similar and contains one additional crystal-field multiplet (CFM) term (D_q) redistributing the energies of the d states:

$$\mathcal{H}_{CFM} = \mathcal{H}_{AM} + \sum_{(2)} D_q d_1^\dagger d_2.$$

The charge-transfer multiplet Hamiltonian is more complex and contains, for example, two configurations for the ground state, in the present case $3d^0$ and $3d^1\bar{L}$. In the calculations only one ligand-hole state is used, in other words the ligand-hole band (\bar{L}) is approximated with one state at a certain energy. The energy difference between a configuration A ($3d^0$) and configuration B ($3d^1\bar{L}$) is indicated as Δ_i . The hybridization between $3d^0$ and $3d^1\bar{L}$ is given with V . We use the convention that $V_{i_{2g}} = 2 \cdot V_{e_g}$. Notice that this is the opposite of the convention used in octahedra¹¹ because CaF_2 has an eightfold cubic surrounding. The charge-transfer multiplet (CTM) Hamiltonian is

$$\begin{aligned} \mathcal{H}_{CTM} = & \sum_A \varepsilon_A A^\dagger A + \mathcal{H}_{CFM,A} \\ & + \sum_B \varepsilon_B B^\dagger B + \mathcal{H}_{CFM,B} \\ & + \sum_{A=B} V_{AB} (A^\dagger B + B^\dagger A). \end{aligned}$$

$A^\dagger A$ gives the occupation of configuration A . The summations are over all possible symmetries within a cubic field. The energy difference $\varepsilon_B - \varepsilon_A$ is defined as Δ . For both the configuration A and B complete crystal-field multiplet calculations are done. The hybridization term

mixes the configurations A and B from identical symmetries. The terms containing U_{dd} and U_{pd} , as given in Ref. 6, are not included explicitly. Within the present notation they only determine the effective energy differences (Δ) between the configurations A and B (see below).

Figure 1 sketches the dipole transition (D_A) and Coulomb matrices (C_A) for the $2p3p3p$ resonant Auger transitions at the Ca $2p$ edge in CaF_2 . C_R denotes the Coster-Kronig decay of the $2p^5 3d^1$ excitonic states to the $2p^5 3d^0 k$ state, further discussed in Sec. III C. In the present analysis we omit the $3s$ photoemission channel which, though strongly coupled,¹² does not influence the shapes of the $2p3p3p$ resonant Auger spectra significantly.¹³ The $2p$ x-ray absorption process to the $2p^5 3d^1$ states has a dipole strength D_A . The initial state is given as $3d^0 + 3d^1\bar{L}$. With $\Delta_i = 9$ eV and $V_{i_{2g}} = 2$ eV, the ground state has for 95% $3d^0$ character. For the $2p^5 3d^1 + 2p^5 3d^2\bar{L}$ intermediate state we have $\Delta_x = \Delta_i + U_{3d3d} - U_{2p3d}$. Extending on the values determined for other transition metal compounds¹⁴ we choose $U_{3d3d} = 4$ eV and $U_{2p3d} = 6$ eV, hence $\Delta_x = 7$ eV.

The $2p^5 3d^1$ states decay via the ($3p3p; 2p\varepsilon_p$) Coulomb matrix element (C_A) to reach the $3p^4 3d^1 \varepsilon_p$ final states. The Coulomb matrix elements to a free electron of f symmetry are not included in the present paper (they are in Ref. 13) but this does not influence the spectral shapes. The same matrix elements couple $2p^5 3d^2\bar{L}$ to $3p^4 3d^2\bar{L}\varepsilon_p$. Because there are two $3p$ holes the value of Δ_f is given as $\Delta_f = \Delta_i + U_{3d3d} - 2 \cdot U_{3p3d}$. With $U_{3d3d} = 4$ eV and $U_{3p3d} = 6$ eV, we find $\Delta_f = 1$ eV. The consequence of this small final state charge-transfer energy is a strong mixing of both configurations. In practice there are five empirical parameters in the present charge-transfer calculations: Δ_i , Δ_x , and Δ_f , as discussed respectively 9, 7, and 1 eV, the hybridization parameter $V_{i_{2g}} = 2$ eV and the cubic crystal-field (D_q) set to -0.45 eV. Note that the crystal-field strength used in a crystal-field multiplet model, -0.9 eV,² is larger than the value used in a charge-transfer multiplet model because in the latter the hybridization

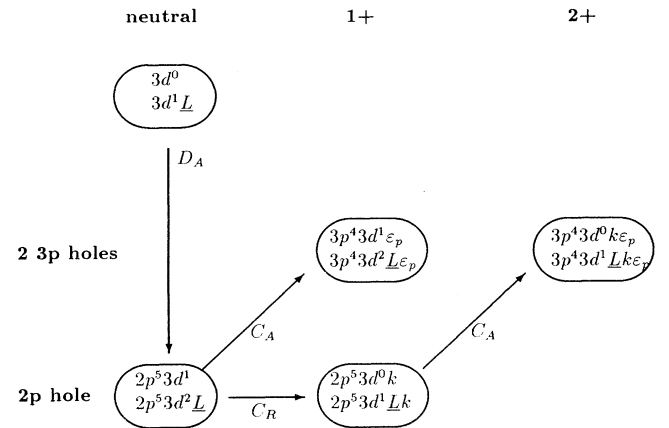


FIG. 1. The configurations used to describe the $2p3p3p$ resonant Auger spectra of CaF_2 . The vertical position gives the core hole indicated on the left. The horizontal position gives the ionization state (see text).

is different for e_g and t_{2g} orbitals causing an additional splitting.¹⁵

Three types of Coulomb interactions occur in the charge-transfer multiplet model: The Auger matrix elements describing the decay of one configuration to another with the escape of a free electron; the Coulomb interactions, or hybridization, coupling two different configurations; the Coulomb interactions coupling the electrons within a configuration, i.e., the multiplet effects.

Important multiplet effects are caused by the large $\langle 2p3d; 2p3d \rangle$ Coulomb (and exchange) matrix elements of the $2p^53d^1$ intermediate state and the $\langle 3p3p; 3p3p \rangle$ and $\langle 3p3d; 3p3d \rangle$ matrix elements of the $3p^43d^1$ Auger final state. Similar matrix elements exist for the $2p^53d^2\bar{L}$ and $3p^43d^2\bar{L}$ configurations. All Coulomb interaction strengths are calculated with an atomic Hartree-Fock-based program.⁷ The calculated Hartree-Fock values are used for the spin-orbit couplings (ζ) of the $2p$, $3p$, and $3d$ states. The Coulomb ($F^{2,4}$) and exchange ($G^{1,3}$) Slater integrals have been reduced to 80% of their theoretical Hartree-Fock value, following atomic spectroscopy.⁷ The $3p3d$ integrals in the final states have been reduced to 72% of their Hartree-Fock value (90% of their atomic value) in order to make the width of the multiplet structure in agreement with experiment. All parameters used are schematically given in Fig. 2.

Figure 3 shows the $2p$ x-ray absorption spectrum calculated for the transition $3d^0 + 3d^1\bar{L} \rightarrow 2p^53d^1 + 2p^53d^2\bar{L}$ (solid line). It is compared with the crystal-field multiplet spectrum (dashed line)² and the experimental CaF_2 spectrum.¹ Good agreement had been obtained if the seven transitions in the crystal-field multiplet are broad-

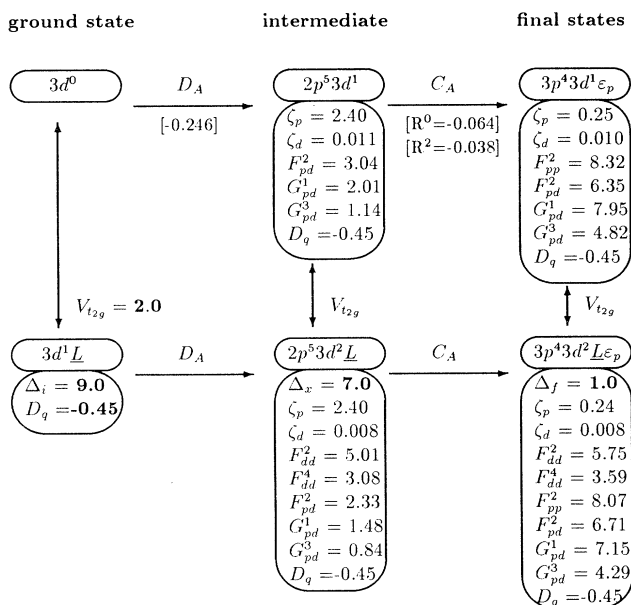


FIG. 2. All configurations and their couplings plus all their parameters as used in the calculation of the $2p3p3p$ resonant Auger spectra of CaF_2 . The dipole transition is given in a.u., the Auger matrix elements (C_A) in a.u. $\text{eV}^{1/2}$. All other parameters are given in eV. The empirical parameters (Δ , V , and D_q) are given in boldface (see text).

ened each with an individual broadening.² In order to lower the number of empirical parameters we have in the present simulations assumed a constant Lorentzian broadening of 0.2 eV for all calculations. The experimental broadening was approximated with a Gaussian with $\sigma = 0.2$. This broadening is approximately correct for the main L_2 peak but it can be seen that it is too large for the other peaks. It is noted that the electron yield spectrum of CaF_2 is affected by intrinsic surface effects which increase the intensity in between the e_g and t_{2g} peaks.²

The four main peaks visible relate, respectively, to the e_g and t_{2g} of the L_3 edge at 347.8 and 349.3 eV, repeated for the L_2 edge at 351.3 eV (e_g) and 352.7 eV (t_{2g}). Apart from these four main peaks three additional peaks are present for the $3d^0 \rightarrow 2p^53d^1$ crystal-field multiplet calculation and many more for the complete charge-transfer multiplet calculation. The open circles denote the excitation energies at which the $2p3p3p$ resonant Auger spectra were measured. The calculations have been done at the same energies.

Figure 4 shows the variations of the theoretical resonant $2p3p3p$ Auger spectral shapes. A remarkable variation is visible in the shape of the resonant Auger spectra. The $2p3p3p$ Auger spectra at the main (or t_{2g}) peaks show most intensity at the highest binding energy in contrast to the e_{2g} peaks which have their maxima at

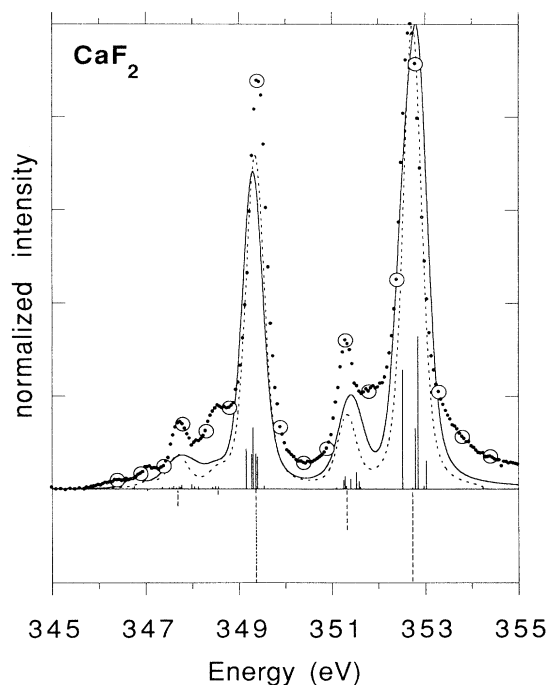


FIG. 3. $2p$ x-ray absorption spectrum of CaF_2 (points). The open circles indicate the excitation energies for the $2p3p3p$ Auger spectra. The solid line is the charge-transfer multiplet simulation and the dashed line the crystal-field multiplet simulation. The individual transitions to final states are given with solid vertical lines. To show the difference more clearly, the crystal-field multiplet calculation is shown negatively.

the low-binding-energy side. Also a difference is visible between L_3 and L_2 , with a higher intensity (at the low-binding-energy side) at the L_2 edge. It can be seen that the $2p3p3p$ resonant Auger spectra have constant binding energy, hence shift with the step energy of 0.5 eV to higher kinetic energy while scanning through the edge. As has been argued in Ref. 1 this behavior is different from normal Auger which has a constant kinetic energy. The reason is that for reaching the same peak in the spectrum, the resonant Auger process is accompanied by a energy change of the $3d^1$ electron. In other words, whatever the energy of the $2p^53d^1$ intermediate state, the energy of the $3p^43d^1$ final state has a constant binding energy.

Figure 5 shows detailed comparisons between experiment and theory for the four main structures of the x-ray absorption spectrum. The theoretical curve for the L_3, t_{2g} peak has been aligned to experiment and all other theoretical spectra are shifted (in kinetic energy) in accordance with their excitation energy. One observes a good agreement of the detailed shape and also of the trends in the relative peak heights at different excitation energies. The t_{2g} spectra show their largest intensity at the lowest kinetic energy. This dominates the L_2, t_{2g} spectrum while for the L_2, e_g spectrum its peak height

is about equal to the peak at the high energy side. This is reproduced in the theory. The L_3, t_{2g} spectrum is correctly reproduced, including the small structure at 293 eV. The dip at 285 eV is deeper in the theoretical curve and there is some uncertainty due to the background at the low energy side. Compared to this the agreement of the L_2, t_{2g} spectrum is worse. For the peaks at 290 and 294 are too high in the theory. A possible reason for this is the presence of normal Auger intensity at 280–285 eV (see discussion). Note that the crystal-field multiplet analysis (Fig. 6.) gives much lower intensity at the low-binding-energy side. Thus it is possible that although the charge-transfer multiplet calculation gives a correct description of the position of the peaks it is (with the parameters used) not perfect for the intensities. The theoretical e_g spectra reproduce the peak maxima at the highest kinetic energy side. Although the general shapes are similar in theory and experiment, the precise structures at the lower kinetic energy side are not in perfect agreement, for example, the theoretical peak in L_3, e_g at 280 eV (and in L_2, e_g at 284 eV) is not distinguishable in experiment. A potentially important factor for this disagreement is the fact that only a single ligand-hole state is included in the calculations and not (as it should in a more complete treatment) a ligand-hole band.

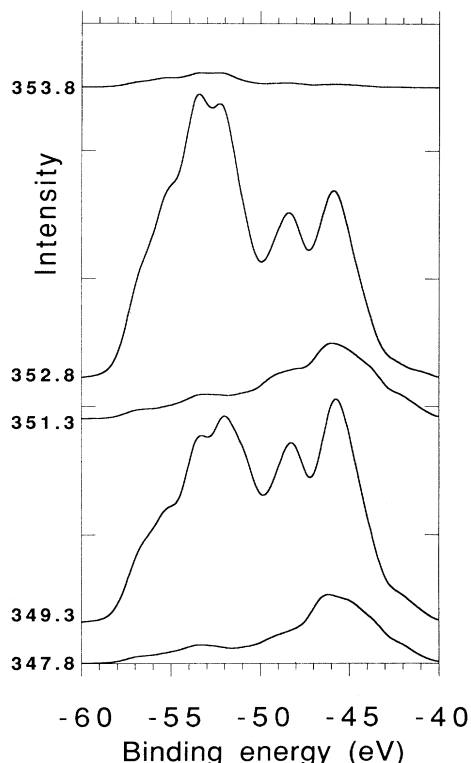


FIG. 4. Simulation of the resonant $2p3p3p$ Auger spectra of CaF_2 . The numbers denote the position in the $2p$ edge as given in Fig. 3. The total intensity of a spectrum is given by the $2p$ x-ray absorption cross section. The spectra taken at the main peaks at 349.3 and 352.8 have been divided by 2. The spectra are given on a binding energy axis to show the same final states at the same energy.

III. DISCUSSION

A. Symmetry effects on the Auger spectral shape

To analyze the symmetry effects in more detail we performed an approximate calculation in which the mixing parameters were set to zero. This identifies with a crystal-field multiplet analysis as has been given already in Ref. 13. This is indicated in Fig. 6. where a comparison is made for the two spectra at (a) the L_3 edge and (b) the L_2 edge. The crystal-field multiplet calculations show much sharper spectra and their agreement with experiment is considerably worse, particularly on the low kinetic energy side. Also the energy difference between the two main peaks is too large. If charge transfer is included the intensity of the peak at -55 eV is smeared out and its maximum is shifted to lower energy. Note that although the spectral shapes are considerably worse for the crystal-field multiplet model, their variation is already in good agreement with the experimental trend. An atomic multiplet calculation (dashed line) is almost identical to the crystal-field multiplet result for the t_{2g} states. This shows that the inclusion of the crystal field is not important for the main peaks. The crystal field is crucial for the small e_g peaks which are absent (the $2p^53d^1$ atomic multiplet consists of only three states²) if the crystal field is not included.

To show the precise nature of the peaks in the $2p$ x-ray absorption spectrum, we have calculated the degree of e_g (t_{2g}) nature of the seven states of the $2p^53d^1$ configurations. Their relative energies, intensities, and purity [degree of e_g (t_{2g}) nature] are given in Table I. The qualitative assignment of the four peaks to, respectively, L_3, e_g , L_3, t_{2g} , L_2, e_g , and L_2, t_{2g} is confirmed in Table I. The pu-

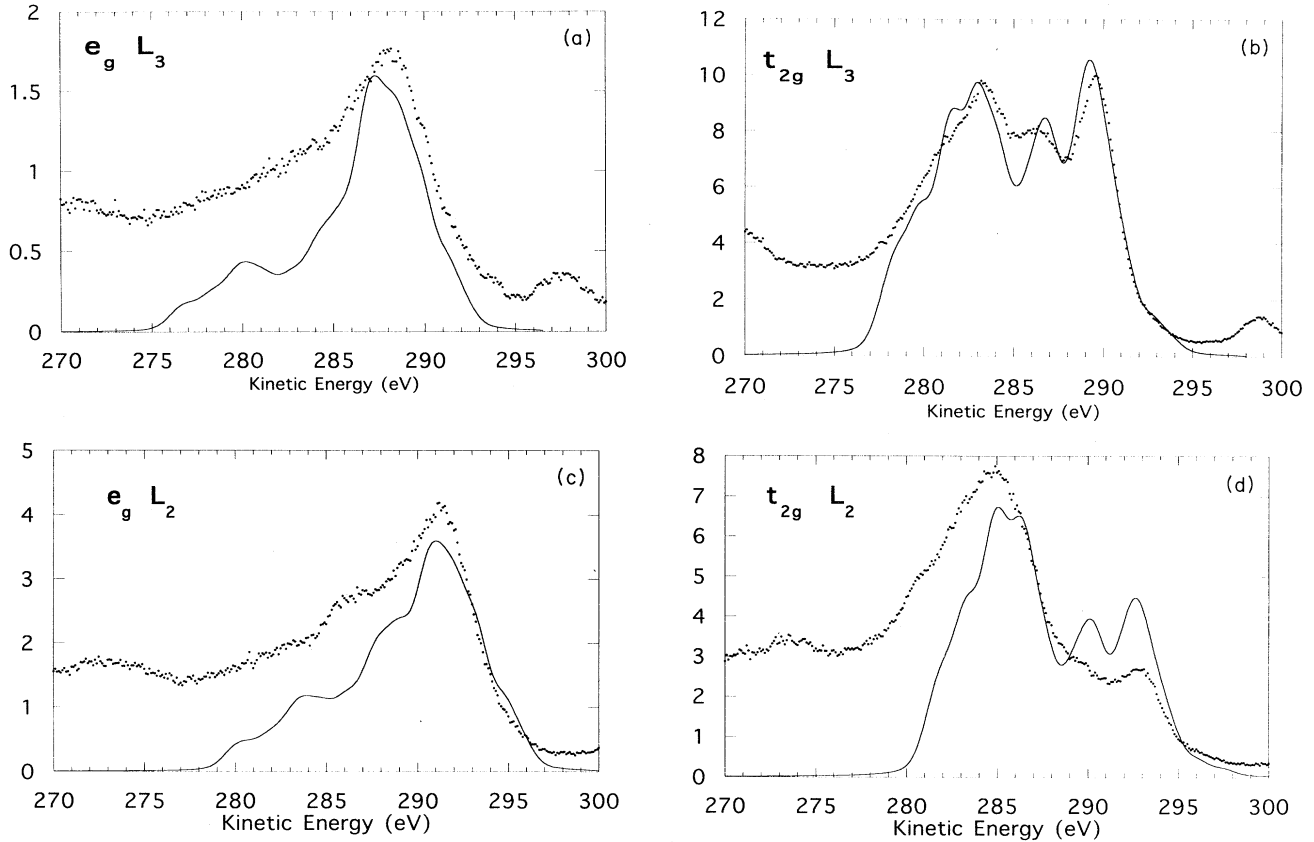


FIG. 5. Comparison between theory and experiment for the four main peaks in the x-ray absorption spectrum. (a) L_3, e_g ; (b) L_3, t_{2g} ; (c) L_2, e_g ; and (d) L_2, t_{2g} . The experimental curves are reproduced from Ref. 1.

rities of the four main peaks are of the order of 60% for the L_3 edge and 70% for the L_2 edge. It is restated that the reason that they are not 100% pure are the multiplet effects.

B. Shake-up versus charge transfer

It was suggested in Ref. 4 that the resonant Auger spectra (of KF) can be separated into normal Auger, shake-up Auger, and spectator Auger. With these three channels the spectra were analyzed, optimising the energies and intensities of the multiplet states in (LS) coupling to the experimental data.⁴ In our analysis as given in Fig. 1, we distinguish only normal Auger (via relaxation to the relaxed $2p^5$ state) and resonant Auger, which can also be called spectator Auger. The shake-up channels seem to have been omitted in our model. However there is an analogy between the $3p^4 4d^1$ shake-up states as discussed in Ref. 4 and the $3p^4 3d^2 \underline{L}$ states in our model. As has been discussed above both the $3d^0$ and $2p^5 3d^1$ states have very little admixture of the ligand-hole states. Due to the presence of two $3p$ holes the two configurations of the final state $3p^4 3d^1$ and $3d^4 3d^2 \underline{L}$ are close in energy, hence strongly mixed. Thus transitions are present from the $2p^5 3d^1$ state to the bonding and also to the anti-

bonding combinations, which gives rise to a satellite. We wish to make an analogy of this satellite with the shake-up peaks in atomic spectroscopy, by noting that shake-up occurs because of “the contraction of the spectator orbital in the course of the decay process.”⁴

A difference between charge transfer and the shake-up channel is that the shake-up (as discussed in Ref. 4) is intra-atomic while charge transfer is interatomic. However the charge-transfer multiplet calculations are in fact performed for a single atom. The ligand-hole states are

TABLE I. Relative energies (in eV), intensities (in \AA^2), and purities (in %) of the seven $2p^5 3d^1$ states as calculated with the crystal-field multiplet model. An asterisk means that the purity of the e_g character given as 94% indicates an expectation value for the crystal-field strength which is 94% of the value reached by a pure e_g state.

Energy	Intensity	Purity
-2.202	0.011	94%* e_g
-1.558	0.067	61% e_g
-1.313	0.003	92% t_{2g}
-0.693	0.026	75% t_{2g}
0.110	0.724	59% t_{2g}
2.077	0.152	75% e_g
3.489	1.014	68% t_{2g}

represented as delocalized d states and the configuration $3d^4 3d^1 + 3d^4 3d^2 \underline{L}$ is represented as $3d^4 3d^1 nd^{10} + 3d^4 3d^2 nd^9$. Note that this formulation really describes intra-atomic mixing of $3d$ and nd . The only difference between an atom and a solid is that the crystal structure of the solid implies a different mixing for t_{2g} and e_g symmetry. Another difference between charge-transfer and the shake-up is that while shake-up describes $3d^N + 3d^{N-1} 4d^1$, the charge-transfer model reads $3d^N + 3d^{N+1} 4d^{-1}$. Thus in both cases a $3d$ electron is exchanged for a $4d$ electron, but the direction is opposite. Despite this paradoxical observation, the analogy between charge transfer and shake-up is that both de-

scribe an initial state as a mixing of $\alpha + \beta$ and a final state as $\alpha' + \beta'$, where due to ionization the contributions of α and β are modified drastically which causes a satellite structure.

C. Resonant versus normal Auger

A last point to discuss is the ratio of resonant versus normal Auger. As discussed above resonant (both spectator and shake-up) Auger has a constant binding energy and varies in shape as has been shown. Normal Auger has a constant kinetic energy and constant shape as it originates from the relaxed $2p^5$ state. One can then decompose the experiment into resonant Auger and normal Auger, for example by subtracting the normal Auger spectra from the spectra taken at resonance.

A problem which occurs is the detailed mechanism of the Coster-Kronig decay process. Within a crystal-field multiplet analysis the dominating Coster-Kronig decay channel (CK_a) is $2p^5 3d^1[\alpha] \rightarrow 2p^5 3d^0[\beta]k$, where k is a continuum electron and in general $[\alpha]$ is a $2p_{1/2}$ state and $[\beta]$ a $2p_{3/2}$ state. The energy difference between the $2p_{1/2}$ and $2p_{3/2}$ edge is only 3.5 eV which is less than the theoretical, binding energy of the $3d$ electron.¹ In other words there seems to be no energy gain in process CK_a , hence no Coster-Kronig decay. That is the energy of the lowest $2p^5 3d^0[\beta]k$ continuum start at an energy E_a above the highest $2p^5 3d^1[\alpha]$ exciton ($E_a > 0$).

Within the charge-transfer multiplet model one forms a $2p^5 3d^1$ state with some admixture of $2p^5 3d^2 \underline{L}$. A new Coster-Kronig decay channel (CK_b) becomes possible: $2p^5 3d^2 \underline{L}[\alpha] \rightarrow 2p^5 3d^1 \underline{L}[\beta]k$. Following the analysis as given by Zaanen and Sawatzky,¹⁶ one finds that the energy gain of this CK_b channel is different. Within the charge-transfer model its energy is $E_b = E_a - U_{dd}$. Because $U_{dd} = 4$ eV and E_a is small, it is very likely that this second process can occur. In this situation that process CK_a is forbidden and process CK_b allowed, the degree of hybridization of the $2p^5 3d^1$ state determines the importance of the Coster-Kronig decay. Another consequence of the inclusion of charge transfer is that in the Coster-Kronig final states the different configurations are mixed which will give states of $2p^5 3d^0 k$ nature a lower energy, thereby opening the CK_a channel. Both the channel CK_b and the hybridization-induced channel CK_a imply that increased hybridization gives increased Coster-Kronig decay, hence a shorter life time.

The additional intensity in the energy range of the normal Auger [280–286 eV (Ref. 1)] in the comparison with theory of the spectral shapes in Fig. 5 might indicate the existence of normal Auger for the L_2 edge. It is difficult to quantify the importance of normal Auger. No clear peaks of normal Auger are present and the situation is made difficult due to the rising background visible in the experiment (Fig. 5). Other uncertainties are the spectral details of the present charge-transfer multiplet simulations and the background present in the normal Auger spectrum itself. Because of these uncertainties we did not attempt to make a quantitative estimate for normal

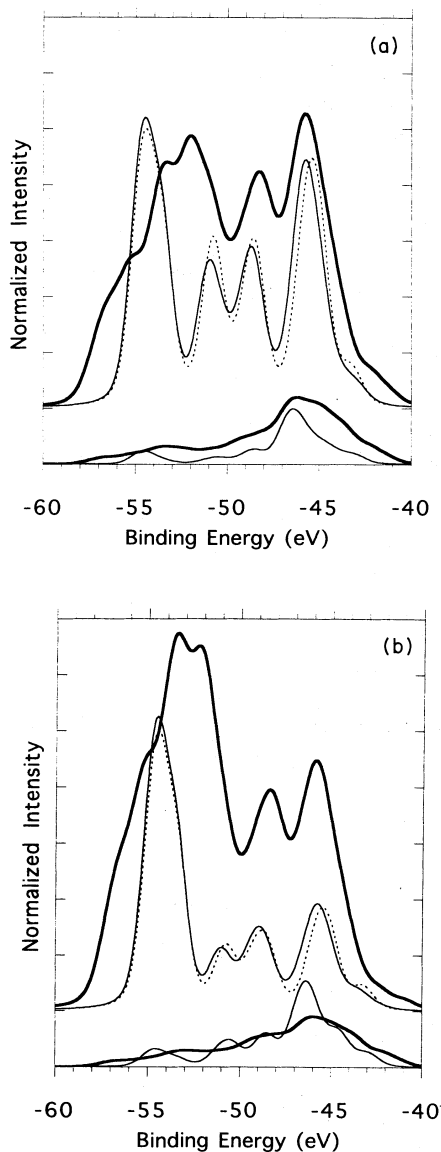


FIG. 6. Top: Comparison for the t_{2g} peaks of (a) L_3 and (b) L_2 of the full charge-transfer multiplet calculations (thick solid lines) with the crystal-field multiplet calculations (thin solid lines) and atomic multiplet calculations (dashed lines). Bottom: same comparison for the e_g peaks.

Auger. We prefer to state that normal Auger, if present, is considerably less important than resonant Auger.

Auger, with for the L_2 edge a potential contribution from normal Auger.

IV. CONCLUDING REMARKS

The $2p3p3p$ resonant Auger spectra of CaF_2 are calculated using a charge-transfer multiplet model. The experimental results are reproduced in detail, indicating that the Auger spectral shape variations are a direct consequence of the symmetries of the intermediate states. The spectra excited at the L_3 edge show only resonant

ACKNOWLEDGMENTS

This work was supported by the European Union programme "Human Capital and Mobility," the Estonian Science Foundation, and the Swedish Institute. We would like to thank Dr. B.T. Thole, Dr. A. Saar, and Dr. A. Kikas for discussions.

* Electronic address: degroot@vsfl.phys.rug.nl

[†] Permanent address: Department of Experimental Physics and Technology, Tartu University, Ulikooli 18, EE2400 Tartu, Estonia.

¹ M. Elango, A. Ausmees, A. Kikas, E. Nommiste, R. Ruus, A. Saar, J.F. van Acker, J.N. Andersen, R. Nyholm, and I. Martinson, *Phys. Rev. B* **47**, 11 736 (1993); A. Kikas, A. Ausmees, M. Elango, E. Nommiste, R. Ruus, and A. Saar, *J. Electron Spectrosc.* **68**, 287 (1994).

² F.M.F. de Groot, J.C. Fuggle, B.T. Thole, and G.A. Sawatzky, *Phys. Rev. B* **41**, 928 (1990); F.J. Himpsel, U.O. Karlsson, A.B. McLean, L.J. Terminello, F.M.F. de Groot, M. Abbate, J.C. Fuggle, J.A. Yarmoff, B.T. Thole, and G.A. Sawatzky, *ibid.* **43**, 6899 (1991).

³ F.M.F. de Groot, *J. Electron Spectrosc.* **67**, 529 (1994).

⁴ E. Kukkk, S. Aksela, H. Aksela, E. Nommiste, A. Kikas, A. Ausmees, and M. Elango, *Phys. Rev. B* **50**, 9079 (1994).

⁵ A. Tanaka and T. Jo, *J. Phys. Soc. Jpn.* **63**, 2788 (1992).

⁶ K. Okada and A. Kotani, *J. Electron Spectrosc.* **62**, 131 (1993); *J. Phys. Soc. Jpn.* **61**, 449 (1992).

⁷ R.D. Cowan, *The Theory of Atomic Structure and Spectra*

(University of California Press, Berkeley, 1981).

⁸ P.H. Butler, *Point Group Symmetry Applications: Methods and Tables* (Plenum Press, New York, 1981).

⁹ K. Okada, A. Kotani, and B.T. Thole, *J. Electron Spectrosc.* **58**, 325 (1992); K. Okada, A. Kotani, H. Ogasawara, Y. Seino, and B.T. Thole, *Phys. Rev. B* **47**, 6203 (1993).

¹⁰ B.T. Thole, G. van der Laan, and P.H. Butler, *Chem. Phys. Lett.* **149** 295 (1988).

¹¹ A. Fujimori, F. Minami, and S. Sugano, *Phys. Rev. B* **29**, 5225 (1984); A. Fujimori and F. Minami, *ibid.* **30**, 957 (1984).

¹² P.S. Bagus, A.J. Freeman, and F. Sasaki, *Phys. Rev. Lett.* **30**, 851 (1973).

¹³ F.M.F. de Groot, *Solid State Commun.* (to be published).

¹⁴ J. Zaanen, C. Westra, and G.A. Sawatzky, *Phys. Rev. B* **33**, 8060 (1986).

¹⁵ The hybridization-induced crystal-field effect can be approximated as $D_q^{\text{HYB}} = \sqrt{(\Delta^2 + 4V^2)} - \sqrt{(\Delta^2 + V^2)}$ (Ref. 3).

¹⁶ J. Zaanen and G.A. Sawatzky, *Phys. Rev. B* **33**, 8074 (1986).